

# Direct measurement of proton straggling in GaAlAs for nuclear profiling

A. H. Bond, P. Parayanthal, and F. H. Pollak

*Physics Department, Brooklyn College of CUNY, Brooklyn, New York 11210*

J. M. Woodall

*IBM Thomas J. Watson Research Center, Yorktown Heights, New York 10598*

(Received 26 September 1983; accepted for publication 3 January 1984)

We present the first direct measurement of proton energy-loss straggling in  $\text{Ga}_{1-x}\text{Al}_x\text{As}/\text{GaAs}$ , enabling us to take maximum advantage of the  $^{27}\text{Al}(p, \gamma)^{28}\text{Si}$  nuclear reaction as a powerful nondestructive technique for measuring Al profiles in these structures. Results were obtained using samples produced by molecular beam epitaxy and fabricated to have step-function Al concentration distributions to prescribed depths. The exact straggling width was obtained by a least-square comparison of the experimental spectra with curves calculated using a parameterized straggling distribution. With these results, profiling measurements can now be made giving the Al concentration fall-off at the GaAlAs/GaAs interface with a spatial depth resolution of about 4% and epilayer thickness determinations to about 2%. We have also observed in one sample a nonabrupt transition at the GaAlAs/GaAs interface, due to differences in substrate surface preparation procedures prior to growth of the GaAlAs layer.

PACS numbers: 61.80.Mk, 68.55.+b, 82.80.-d, 66.30.-h

The GaAlAs/GaAs heterostructure interface is currently of considerable interest because of its application in such devices as cw room temperature lasers, quantum well lasers, modulation doped high electron mobility transistors (HEMT), high efficiency solar cells, etc. For such structures, as well as recently developed heterojunctions such as the GaAlSb/GaSb system,<sup>1</sup> the distribution of Al in the epilayer and at the interface is an extremely important characterization parameter. In the past, Al profile measurements have been made by techniques such as secondary ion mass spectroscopy<sup>2</sup> and Auger electron spectroscopy,<sup>3</sup> involving removal of layers of the material by procedures such as ion milling, which may introduce experimental artifacts. Profile measurements have also been made by Rutherford backscattering<sup>4</sup> which does not have a very high resolution for the GaAlAs system.

Recently, a nondestructive technique for profiling Al in these structures has been developed<sup>5</sup> utilizing the  $^{27}\text{Al}(p, \gamma)^{28}\text{Si}$  nuclear reaction. The method takes advantage of an extremely sharp ( $\approx 100$  eV) resonance in the cross section for the reaction, occurring at a proton energy of 992 keV. At higher incident energies, protons penetrate the sample, losing energy until at some depth they pass through the resonant energy, producing 10.7 MeV  $\gamma$  rays in proportion to the concentration of Al at this depth. Depth profiling is thus accomplished by varying the energy of the incident proton and measuring the yield of the emitted  $\gamma$  rays.

In order to take maximum advantage of the precision of nuclear profiling as a characterization method, it is necessary to know accurately the limitations on the depth resolution of the technique. The conversion of the measured yield versus proton energy into a depth profile of Al concentration requires an accurate knowledge of three effects: the mean energy loss process, the initial energy resolution of the proton beam, and the energy broadening mechanism of straggling, which results from the statistical nature of the energy loss mechanism. Thus, the protons at a given depth in the

sample are not monoenergetic but instead have an approximately Gaussian distribution of energies whose width is an increasing function of depth. The straggling affects the profile measurements as would an instrumental resolution broadening, i.e., the apparent sharpness of any Al concentration gradient as reflected in the measured  $\gamma$ -ray yield is reduced due to convolution of the profile with the straggling distribution. Although several experimental studies<sup>6,7</sup> of straggling exist, inconsistencies in straggling parameters measured in different laboratories are as high as 30%. Furthermore, no experimental studies of straggling in GaAlAs have been made. Also, since one recent theoretical study<sup>8</sup> predicts complex fluctuations in the value of the straggling parameter as a function of atomic number, the method of estimating the straggling parameter in GaAlAs by interpolating between measured values in nearby elements in the periodic table is questionable. In the previous profiling work<sup>5</sup> in GaAlAs, corrections for straggling were based on a simplified procedure involving the use of a straggling width estimated theoretically rather than experimentally determined in the material itself, and involving the use of the derivative of the measured yield to extract the widths of the yield function at the GaAlAs/GaAs interface, rather than a deconvolution of the integral of the profile with an appropriate resolution function.

In this communication we present the first direct measurement of straggling in  $\text{Ga}_{1-x}\text{Al}_x\text{As}/\text{GaAs}$ , enabling us to measure the sharpness of the Al concentration fall-off at the interface with a spatial depth resolution of about 4% of the epilayer thickness, and to determine the thickness of the epilayer itself with an accuracy of about 2%. These results were obtained using samples produced by molecular beam epitaxy (MBE) and fabricated to have step-function Al concentration profiles to prescribed depths. The  $\gamma$ -ray yield distribution from these samples was compared with a function obtained by convoluting the appropriate step function with a parameterized straggling distribution corrected for the ini-

tial energy spread of the proton beam. The exact straggling parameter was obtained by a least-square fit of this function to the data.

Displayed in Fig. 1 is a schematic of the experimental setup. A monoenergetic proton beam having an energy a few keV above the 992 keV resonance value impinges upon the sample which is in a vacuum chamber at about  $10^{-6}$  Torr. The beam energy is determined by magnetic analysis and its calibration and resolution energy spread was found to be 2.8 keV full-width at half-maximum (FWHM). At some depth in the sample, determined by the incident beam energy, the beam reaches the resonant energy, producing 10.7 MeV  $\gamma$  rays which are detected by a  $3 \times 3$  in. NaI detector located just outside the vacuum chamber. Typical beam current intensities were 250 nA and detector counting rates were of the order of 1–10 counts/s. The beam spot on the sample was about 1.5 mm in diameter.

The three samples used in this study were GaAlAs/GaAs structures grown by MBE with various epilayer thicknesses. Two of the samples were fabricated with MBE grown GaAs buffer layers, while the third was grown directly onto the GaAs substrate. For sample MBE 31-3 a buffer layer of *p*-GaAs ( $\approx 1 \mu\text{m}$ ), followed by a layer of *n*-GaAs substrate ( $\approx 5000 \text{ \AA}$ ) was grown on an *n*-type substrate at  $600^\circ\text{C}$ . This was followed by a GaAlAs epilayer ( $\approx 1000 \text{ \AA}$ ). For MBE 32-X, the epilayer of GaAlAs ( $\approx 4000 \text{ \AA}$ ) was grown on a semi-insulating GaAs substrate on which two buffer layers of GaAs—one *p* type ( $\approx 1.5 \mu\text{m}$ ) and the other *n* type ( $\approx 2 \mu\text{m}$ ) was grown by MBE at  $550^\circ\text{C}$ . In preparing MBE 49-4, the epilayer was grown directly onto a *p*-type GaAs substrate, which was thermally cleaned without excess As. The MBE procedures used for all samples were designed to produce abrupt interfaces between the GaAlAs and GaAs re-

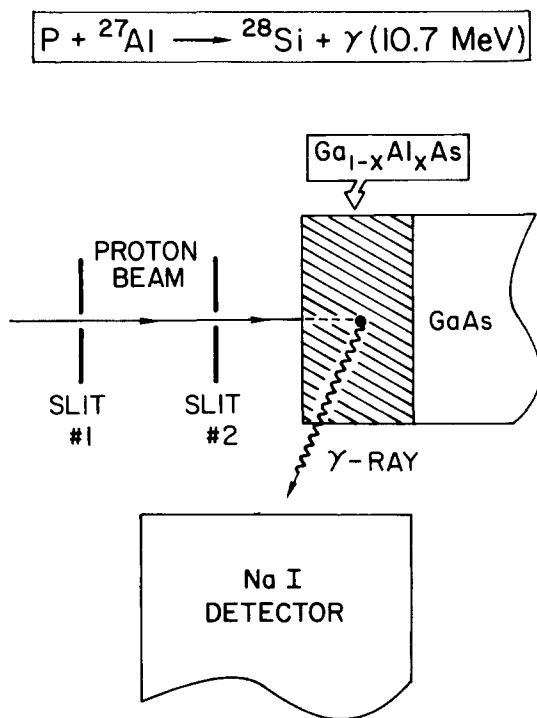


FIG. 1. Schematic representation of the experimental arrangement.

gions. The composition  $x$  was evaluated by Raman scattering<sup>9</sup> and found to be 0.4 for samples MBE 31-3 and MBE 32-X and 0.5 for sample MBE 49-4. These values are consistent with the growth conditions.

Figures 2(a) and 2(b) show the profile data, indicated by dots, on the two MBE samples, MBE 31-3 and MBE 32-X, respectively, plotted as  $\gamma$ -ray yield versus incident proton energy  $E_0$ . In order to calculate the energy lost by the proton beam in traversing a given thickness of sample, the stopping power data compiled by Anderson and Ziegler<sup>10</sup> was used, and Bragg's rule was employed to calculate the stopping power for the composite material. The depth  $z(E_0)$ , indicated at the top of the figure, was then calculated for which the energy loss was equal to the difference between  $E_0$  and the resonance energy  $E_r$ . The  $\gamma$ -ray yield as a function of  $E_0$  can then be translated into Al concentration as a function of  $z$ . The profile thus obtained, however, cannot be compared directly with the actual distribution of Al in the sample because of two effects, energy-loss straggling and incident beam energy spread, which broaden the measured profile.

First, the effect of energy-loss straggling, resulting from the statistical nature of the energy-loss process, produces an approximately Gaussian distribution for the energy of the proton beam at a given mean energy depth. Most theoretical calculations agree that for a given material and for losses small compared with  $E_0$ , the width  $\Delta_s$  of this distribution

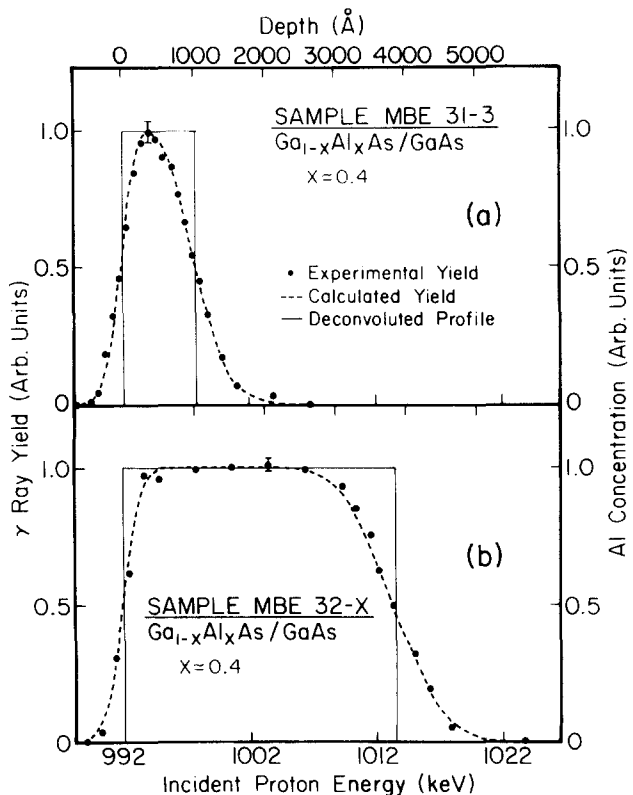


FIG. 2. (a) and (b)  $\gamma$ -ray yield (in arbitrary units) as a function of incident proton energy for two MBE grown samples, MBE 31-3 and MBE 32-X. The data are indicated by dots. Representative error bars are shown. The dashed lines represent best-fit curves to the data calculated from Eq. (3) using step-function profile distributions represented by the solid lines. The scale at the top of the figure represents the depth corresponding to a given incident proton energy.

should increase proportionally with the square root of the depth  $z$ , although the proportionality constant differs somewhat in various theoretical models. The simplest of these theories, the Bohr theory,<sup>11</sup> predicts that this width should be given by the formula

$$\Delta_B = (8\pi e^4 Z_1^2 Z_2 N z)^{1/2} = K_B z^{1/2}, \quad (1)$$

where  $Z_1$  and  $Z_2$  represent the projectile and target atomic numbers, respectively, and  $N$  is the atomic density of the target. Several more recent theories of straggling exist, taking into account the atomic structures of the target material. These theories also predict the same simple relationship between depth  $z$  and the straggling  $\Delta_s$ , namely,

$$\Delta_s = K z^{1/2}, \quad (2)$$

but differ from the Bohr theory in predicting a somewhat lower value for  $K$ , especially for  $Z_2 > 10$ . Furthermore, theoretical calculations by Chu predict an oscillatory behavior of  $K$  as a function of  $Z_2$ , due to atomic shell effects. In addition to straggling, there is a contribution  $\Delta_0$  to the broadening due to the energy spread of the incident proton beam. This effect broadens the measured profile at the sample surface as well as at a depth  $z$ . This incident energy spread was extracted from profile measurements on a thick Al target. The slope of the  $\gamma$ -ray yield from this target as a function of  $E_0$  near  $E_0 = E_r$  offered a direct measurement of  $\Delta_0$ , which was found to be 2.8 keV FWHM.

In order to extract the straggling width  $\Delta_s$  from the data, a theoretical yield  $Y(E_0, z_0, \Delta_s)$  was calculated from the integral

$$Y(E_0, z_0, \Delta_s) = A \int_0^\infty dz \rho(z) [\Delta_0^2 + \Delta_s^2(z)]^{-1/2} \times \exp - \{ [E_r - \bar{E}(z)]^2 / [\Delta_0^2 + \Delta_s^2(z)] \}, \quad (3)$$

where  $\bar{E}(z)$  is the mean beam energy at depth  $z$  and  $\rho(z)$  is the Al depth distribution (in the sample). For the samples in Fig. 2,  $\rho(z)$  was assumed to be a step function of thickness  $z_0$ . This theoretical yield  $Y(E_0, z_0, \Delta_s)$  was then compared with the experimental  $\gamma$ -ray yield  $Y(E_0)$  using a least-squares calculation which allowed both  $z_0$  and  $\Delta_s$  to vary independently. Thus, both the epilayer thickness and the straggling width  $\Delta_s$  could be obtained from the experimental data. The dashed lines in Fig. 2 represents the best-fit value of  $Y(E_0)$  using this procedure. The solid lines represent the resultant step-function profiles used in generating these best-fit curves. Agreement between  $Y(E_0)$  and the experimental points is quite good.

Table I tabulates the results, presented as best-fit values of the straggling width  $\Delta_s$  and epilayer thickness  $z_0$  for sam-

TABLE I. The measured straggling coefficient ( $K_M$ ) and thickness for the two samples MBE 31-3 and MBE 32-X. The ratio  $K_M/K_B$ , where  $K_B$  is the Bohr straggling coefficient, is also listed.

Sample	Thickness (Å)	$K_M$ (eV Å <sup>-1/2</sup> )	$K_M/K_B$
MBE 31-3	1080 ± 20	72.0 ± 3.6	0.89 ± 0.05
MBE 32-x	3880 ± 80	68.3 ± 1.4	0.84 ± 0.02

ples MBE 31-3 and 32-X. In the third column, the measured coefficient  $K_M$  from Eq. (2) is presented, and in the fourth column  $K_M$  is compared with  $K_B$ , the coefficient calculated from the Bohr theory [Eq. (1)]. The consistency of  $K_M$  for the two samples confirms the  $z^{1/2}$  dependence of  $\Delta_s$ , and the fact that  $K_M$  is somewhat smaller than  $K_B$  is consistent with more recent calculations. The experimentally determined thickness for both samples is in good agreement with that predicted from the growth conditions.

Figure 3 shows the profile data on sample MBE 49-4. For this sample, the transition region could not be fit assuming a step-function distribution for  $\rho(z)$  and using the same deconvolution procedure and straggling parameter as for the previous two samples. The data indicated a nonabrupt transition at the interface in this sample. The transition line giving the best fit to the data, after convolution with the straggling function and initial beam broadening, is represented by the solid line in Fig. 3 and indicates an interfacial region of approximately 2000 Å in width for this sample. The nonabruptness of the Al gradient in this sample is probably due to differences in stoichiometry between the substrate surface which is thermally cleaned without excess As and the MBE grown GaAs surfaces (samples MBE 31-3 and MBE 32-X) which were grown under excess As, and also had a shorter exposure time prior to growth of the GaAlAs layer. This nonabrupt interface is similar to that seen for GaAlAs layers grown on GaAs by liquid phase epitaxy.<sup>5</sup> The experimentally determined thickness for this sample is also in good agreement with that predicted from the growth conditions.

In conclusion, we have made the first direct measurements of proton straggling in GaAlAs for nuclear profiling, making it possible to realize the full potential of this powerful characterization technique. Thus, profiling measurements can now be made giving the Al concentration fall-off at the GaAlAs/GaAs interface with a spatial depth resolution of about 4% and epilayer thickness determinations to about 2%. We have used the abruptness of the transition

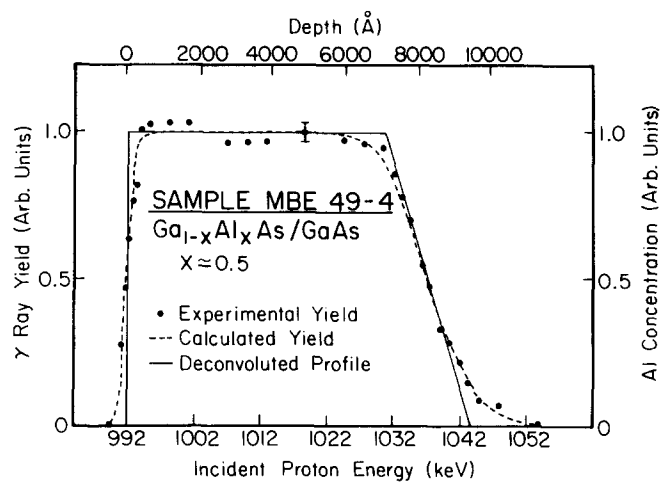


FIG. 3.  $\gamma$ -ray yield (in arbitrary units) as a function of incident proton energy for MBE grown sample MBE 49-4. The data are indicated by dots. A representative error bar is shown. The dashed line represents the best-fit curve to the data calculated from Eq. (3) using the profile distribution represented by the solid line. The scale at the top of the figure represents the depth corresponding to a given proton energy.

region made available by the MBE technique to construct step-function Al concentration distributions and to compare the measured profiles from these samples with a convolution of the appropriate step function with a parameterized straggling distribution corrected for the energy spread of the incident proton beam. Values for the straggling parameter were obtained by a least-square fit of this function to the data for each sample. We have demonstrated the  $z^{1/2}$  dependence of the straggling width, enabling a reliable estimate of the straggling to be made at other depths. The measured straggling parameter is in agreement with recent calculations predicting straggling widths somewhat less than those calculated from the Bohr theory. We have also observed that the condition of the GaAs surface prior to the growth of the GaAlAs layer can affect the abruptness of the interface in these structures.

We gratefully acknowledge the IBM Shared University Research (SUR) Program for its support of this project. One

of us (A.H.B.) wishes to acknowledge the support of PSC/BHE Grant No. 6-63269.

<sup>1</sup>H. Temkin and W. T. Tsang, presented at the 1983 Electronic Materials Conference, Burlington, Vermont.

<sup>2</sup>See, for example, W. K. Chu, M. A. Nicolet, J. W. Mayer, and C. A. Evans, *J. Anal. Chem.* **46**, 2136 (1974).

<sup>3</sup>See, for example, C. M. Garner, C. Y. Su, and W. E. Spicer, *J. Vac. Sci. Technol.* **16**, 1521 (1979); P. S. Ho, *Surf. Sci.* **85**, 19 (1979).

<sup>4</sup>See, for example, R. Sahia, J. S. Harris, D. D. Edwell, and F. H. Eisen, *J. Electron. Mater.* **6**, 645 (1977) and references therein.

<sup>5</sup>J. S. Rosner, P. M. S. Lesser, F. H. Pollak, and J. M. Woodall, *J. Vac. Sci. Technol.* **19**, 584 (1981).

<sup>6</sup>See, for example, J. M. Harris and M. A. Nicolet, *Phys. Rev. B* **11**, 1013 (1975).

<sup>7</sup>See, for example, M. Luomajarvi, A. Fontell, and M. Bister, in *Ion Beam Surface Layer Analysis*, edited by O. Meyer, G. Linkes, and F. Kappler (Plenum, New York, 1976), p. 75.

<sup>8</sup>W. K. Chu, *Phys. Rev. A* **13**, 2057 (1976).

<sup>9</sup>P. Parayanthal, F. H. Pollak, and J. M. Woodall, *Appl. Phys. Lett.* **41**, 961 (1982).